Article

Not peer-reviewed version

Impact of High-Shear Homogenization Pretreatment on Process Productivity, Economic Feasibility, and Product Quality During Long-Term Crossflow Microfiltration of Andean Blackberry Juice

Pablo Rodríguez *, Juan Zuluaga, Santiago González, Victoria Escobar, Misael Cortés, Fabrice Vaillant

Posted Date: 2 June 2026

doi: 10.20944/preprints202606.0231.v1

Keywords: Andean blackberry juice; non-thermal juice processing; crossflow microfiltration; high-shear homogenization; flux decline kinetics; regime analysis; techno-economic feasibility

 doi:10.20944/preprints202606.0231.v1

Article

Impact of High-Shear Homogenization Pretreatment on Process Productivity, Economic Feasibility, and Product Quality During Long-Term Crossflow Microfiltration of Andean Blackberry Juice

Pablo Rodríguez [1,*], Juan Zuluaga [2], Santiago González [1], Victoria Escobar [1,2], Misael Cortés [2] and Fabrice Vaillant [1,3,4]

[1] Corporación Colombiana de Investigación Agropecuaria-Agrosavia, Centro de Investigación La Selva, Agrosavia, Colombia
[2] Departamento Ingeniería Agrícola y Alimentos, Facultad Ciencias Agrarias, Universidad Nacional de Colombia, Medellín, Colombia
[3] French Agricultural Research Centre for International Development (CIRAD), UMR Qualisud, Rionegro, Antioquia, Colombia
[4] Joint Research Unit—UMR Qualisud, Univ Montpellier, Avignon Universite, CIRAD, Institut Agro, IRD, Universite de La Reunion, Montpellier, France
* Correspondence: prodriguezf@agrosavia.co; pabloerf@gmail.com; Tel: +573176582802

Abstract

Andean blackberry is a highly perishable fruit rich in anthocyanins and ellagitannins, and its short postharvest life significantly affects smallholder growers' economies. Although crossflow microfiltration is a promising non-thermal stabilization technology for blackberry juice, its industrial application is limited by permeate flux decline during long-term operation, while most previous studies have focused on short processing times. This study evaluated the effect of high-shear homogenization prior to enzymatic depectination on flux decline, product quality, and techno-economic feasibility during CFM. Juice processed by conventional grinding followed by high-shear homogenization and enzymatic treatment was subjected to CFM at feed volumes up to 400 L and volumetric reduction factors close to 30. Homogenization significantly reduced particle size and suspended insoluble solids, resulting in higher permeate flux, improved flux stability, and greater productivity. Flux decline analysis showed that high-shear homogenization extended the stable filtration regime and delayed severe fouling, sustaining higher average permeate fluxes during long-term operation. Product quality was preserved, ensuring microbial reduction while improving anthocyanin and ellagitannin recovery and enhancing blackberry aroma. In addition, HS3+E reduced energy consumption and beverage production cost while achieving a positive NPV and a 21% IRR. Overall, homogenization improved the industrial feasibility of long-term CFM processing of Andean blackberry juice.

Keywords: Andean blackberry juice; non-thermal juice processing; crossflow microfiltration; high-shear homogenization; flux decline kinetics; regime analysis; techno-economic feasibility

1. Introduction

Andean blackberry (*Rubus glaucus* Benth.), is an important perennial fruit cultivated across the Andean highlands of Colombia and Ecuador, where it is predominantly grown by smallholder farmers on plots often smaller than 1 ha, contributing significantly to rural employment and household income while supporting local fresh and processing markets. However, this fruit is highly

 doi:10.20944/preprints202606.0231.v1

perishable, exhibiting rapid softening and susceptibility to microbial spoilage shortly after harvest, with fresh fruits maintaining acceptable quality for only a few days under ambient conditions and up to approximately 8 days under refrigeration before quality declines due to firmness loss and microbial growth [1].

Despite these challenges, Andean blackberry is recognized for its rich phytochemical profile, including high levels of anthocyanins, ellagitannins, and other phenolic compounds associated with antioxidant, anti-inflammatory activity and others potential health benefits. The combination of short postharvest life and high functional value underscores the need for effective gentle processing technologies to reduce postharvest losses and preserve phytochemical quality while enhancing market opportunities for small-scale growers [2]

Thermal pasteurization (LTLT or, more commonly used for juices, HTST) is widely used to ensure microbial safety and extend shelf life of fruits. However, the literature consistently shows a quality trade-off: heating accelerates degradation of thermolabile bioactive compounds (BAC), particularly anthocyanins, through mechanisms that lead to pigment loss, browning, and changes in the overall phenolic profile. These changes can reduce antioxidant capacity and modify the characteristic "fresh fruit" sensory taste and flavor of berry juices [3]. Studies in dark-colored berry matrices (e.g., blackberry) report measurable decreases in anthocyanins after pasteurization, while some phenolic families can be more stable depending on time–temperature intensity (e.g., ellagitannins sometimes showing higher retention than anthocyanins) [4]. These compositional shifts are frequently associated with sensory impacts, mainly via color changes and aroma/taste differences, which are key drivers of consumer perception [5]. From an investment and operating-cost perspective, pasteurization (HTST) remains advantageous at large industrial scale; however, its energy demand and total cost of ownership depend strongly on heat-exchange design, pumping requirements, and heat recovery/regeneration efficiency [6]

These factors can become critical constraints for the adoption of this process in small and medium agroenterprises, where access to capital investment, maintenance capacity, and energy resources are often limited. Although CFM has demonstrated clear advantages as a mild stabilization technology for fruit juices [7], [8], and recent advances such as flux optimization through backpulsing have been reported, these studies have been restricted to short-term operations (≈1 h) and low volume reduction factors (VCR ≈ 11) [9]. Furthermore, while integrated ultra-clean packaging systems have been proposed [10], the long-term industrial performance of CFM for Andean blackberry juice remains largely unexplored, representing a critical knowledge gap. Under extended operating conditions typical of industrial work shifts, key limiting phenomena such as membrane fouling and cake layer formation may be exacerbated, leading to significant flux decline and potentially compromising process viability. In this context, the novelty of this work lies in evaluating CFM performance under prolonged, industry-relevant conditions. Although it has been reported that particle size distribution and suspended solids significantly influence CFM productivity and fouling behavior [11], there are no studies evaluating these effects under long-term operational conditions representative of industrial processing. Therefore, the objective of this study was to assess the effect of homogenization as a physical pretreatment prior to microfiltration on process productivity, retention of bioactive compounds, sensory attributes, and economic feasibility during the crossflow microfiltration of Andean blackberry juice under extended operating conditions representative of industrial-scale production.

2. Materials and Methods

2.1. Raw Material

Andean blackberry (*Rubus glaucus* Benth.) fruits were harvested at commercial maturity stages 5 and 6 (maturity index ranging from 2.6±0.2 to 4.8±0.2, according to NTC 4106). The fruits were supplied by smallholder farmers' association ASOFRUTAS (La Ceja, Antioquia, Colombia). The

 doi:10.20944/preprints202606.0231.v1

studied was carried out at the agro-industrial pilot plant of the La Selva Research Center (Rionegro, Antioquia, Colombia).

2.4. Andean Blackberry CFM Process

As an initial approach, a backpulsing strategy was evaluated following the methodology reported by Zuluaga et al., [9], however, this condition led to membrane damage under the operating conditions tested. Therefore, subsequent experiments did not include backpulsing as part of the CFM process configuration. Instead, the study focused on physical pretreatments aimed at reducing particle size. In this context, homogenization was selected as the main pre-treatment strategy. Also, a preliminary study was conducted to assess whether pre-treatment affected the sensory quality of the juice.

Two particle size reduction systems were evaluated: a rotor–stator colloidal mill (CM-60, Centricol, Colombia) and a rotor-stator high shear homogenization tri-emulsifying pump (TRL-L3-60, Wenzhou Rayen Machinery Co., Ltd., China), powered by a 4.0 kW Siemens motor operating at 2900 rpm, referred to as HS3. The preliminary results showed that samples processed with the colloidal mill exhibited a pronounced astringent taste, identified as a key factor for consumer rejection. Therefore, subsequent experiments were conducted using the HS3 system.

To evaluate the impact of homogenization on microfiltration performance, two feed preparation strategies were implemented. In the first treatment, called as unit operation Grinder (GR, see figure 1), fruits were mechanically milled using a disc mill (Javar M32I) equipped with a 4.5 mm gap opening. In the second treatment the milled pulp was subjected to high-shear homogenization using a HS3. Temperature during homogenization was controlled below 30 °C using a 20 L recirculating chiller (Centricol Co., Colombia) (see purple dotted line figure 1). Homogenization was performed at a pulp-to-water mass ratio of 7:3 with a recirculation time of 7 min.

Following size reduction, the mixture underwent enzymatic depectinization in a double-jacketed vessel with temperature control (GAME Co., Medellín, Colombia) at 35 °C for 1 h under continuous agitation (See EL figure 1). A commercial multi-enzyme preparation (Pectinex® Ultra SP-L; Modernist Pantry LLC, USA), containing pectinases, hemicellulases, and β-glucanases derived from *Aspergillus aculeatus* (declared activity: 3300 PGNU·g^{-1}), was added at 150 ppm (w/w).

The enzymatically treated mash was then pressed (HP Figure 1) using a vertical hydraulic press (300 L; Enotecnica Pillan, Vicenza, Italy) fitted with a 1.2 mm external mesh and an expandable internal membrane, applying a maximum pressure of 300 kPa for juice ex-traction. The resulting press cake was washed and re-pressed in two additional cycles to maximize the recovery of soluble bioactive compounds from drupe tissues and residual solids.

 doi:10.20944/preprints202606.0231.v1

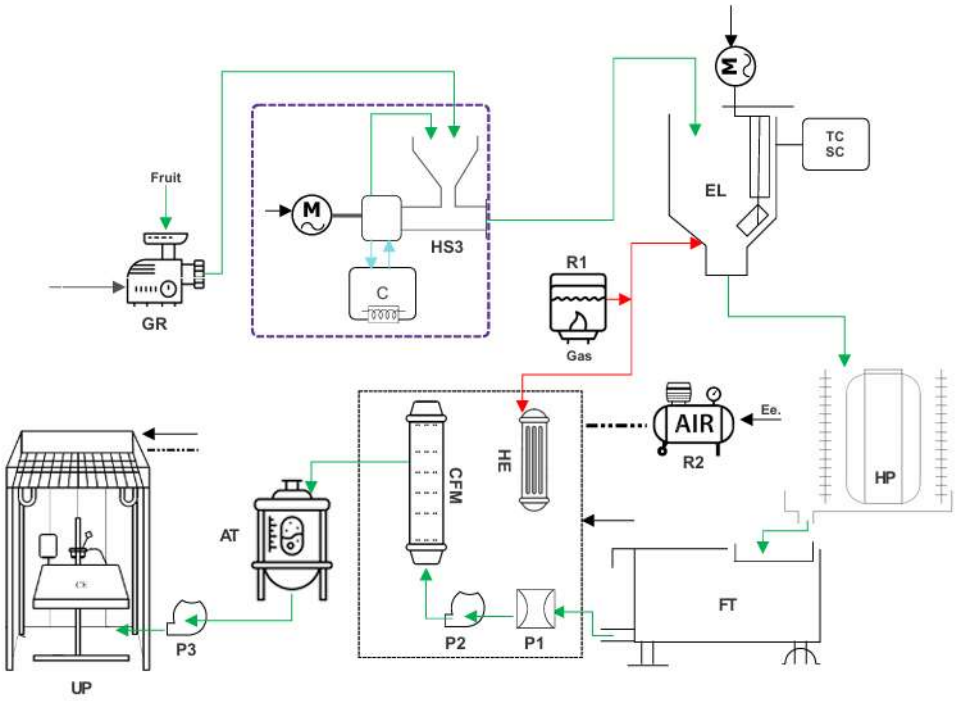

GR	disc mill	**HP**	hydro press	**CFM**	cross flow microfiltration module
HS3	homogenizer	**TC**	temperature control	**HE**	heat exchanger
C	recirculating Chiller	**SC**	speed control	**AT**	aseptic tank
R1	steam boiler	**FT**	formulation / feed tank	**UP**	filling system
R2	air compressor	**P1**	diaphragm pump		
EL	enzymatic liquefaction vessel	**P2**	centrifugal pump		

Figure 1. Integrated CFM process line to produce Andean blackberry juice. Line conventions: green lines indicate product flow; red lines indicate steam supply; blue lines indicate water circulation; black lines indicate electrical energy; dashed lines indicate compressed air.

To obtain formulated raw juice with 40% fruit content, water was added to a 400 L feed tank (FT figure 1) at a volume equivalent to twice the initial mass of the raw material. Total soluble solids (TSS) were adjusted to 10.5 °Brix by adding approximately 7% (w/w) sugar.

The CFM unit (gray dotted square, see Figure 1) was locally built (GAME Co., Medellín, Colombia) and consisted of a double-diaphragm pump (P1 figure 1) (SaniForce® 515) used for pressurized raw juice feed supply, and a centrifugal pump (P2 figure) (QIS series, 7.5 HP; 50/60 Hz) used to generate a tangential flow velocity of 6 $m \cdot s^{-1}$. Microfiltration was performed using a module equipped with three tubular ceramic membranes (CFM Figure 1) (α-Al_2O_3, Membralox GP-IC EP4840, Bazet, France). Each membrane contained 48 channels with an internal diameter of 4.0 mm and a nominal pore size of 0.2 µm. The membranes, each 1020 mm in length, were vertically installed within the module, providing a total effective filtration area of 1.8 m^2 and sealed with elastomeric EPDM gaskets. The permeate flow rate was continuously monitored using an electromagnetic flowmeter (Sitrans f m mag 5000, Siemens).

All experiments were conducted in continuous feed mode without retentate withdrawal. System temperature was maintained at 35 °C using a shell-and-tube heat exchanger (HE figure). Feed pressure (Pf) and permeate pressure (Pp) were measured using diaphragm pressure gauges to maintain a constant trans-membrane pressure (TMP) of 150 kPa [9]. Flow circulation and operational parameters were controlled via solenoid valves connected to a programmable logic controller (PLC Xinje TG765-UT) and operated using an HMI touchscreen interface. The permeate was collected in an aseptic tank (AT, Figure 1) coupled to an ultra-clean packaging system (UP, Figure 1) consisting

 doi:10.20944/preprints202606.0231.v1

of a laminar airflow cabinet equipped with a HEPA 0.3 um filter and a semi-manual filling machine (Sympaty TOP 320®) with an AL40 side-channel pump (P3, Figure 1). The Andean blackberry micro filtrated juice was immediately packed into pre-irradiated multilayer bags (LDPE/metallized PET/LDPE; FLEXBAG, Santa Anita, Lima, Peru), equipped with V-pull valves.

2.4.1. Membrane Cleaning in Place (CIP) Procedure

The CIP sequence consisted of an initial rinse with neutral water, followed by two alkaline cleaning cycles using a 1.5% (w/w) NaOH solution at 90 °C for 20 min. Subsequently, an acidic treatment was performed using a 1% (w/w) HNO_3 solution at 90 °C for 20 min. The protocol concluded with a final neutralization rinse. The cleaning procedure was carried out according to established membrane cleaning guidelines [12]. The permeate piping and aseptic tank were sterilized with steam at 210 kPa during 20 min, while pressure was regulated using a vent filter (PES, 0.2 μm).

2.5. Process Productivity

2.5.1. Permeate Flux (Jp_x)

The permeate flu (Jp_x) was determined from the volume of permeate collected (V_p, L), the total membrane filtration area (A, m²), and the effective operating time (t, h), according to [13] as expressed in Equation (1):

$$J_{px} = \frac{V_p}{A*t} \quad \text{(Eq. 1)}$$

To fit the flowmeter data to the experimental work volumes (instant flux), to avoid overestimated values, the Jp_x values were trending by the gel-polarization model, a mechanistic model often used for the adjustment of experimental data as a function of the logarithm of VCR according to eq 2 [9] Zuluaga et al 2024

$$Jp_{inst} = Kc\, Ln\left(\frac{cg}{cb}\right) \quad \text{(Eq. 2)}$$

where *Kc* represents the overall mass transfer coefficient, (cg/cb) is the ratio between concentration of retained material in the bulk of retentate (cb), and the concentration at the membrane interface (cg). cg is a constant, characteristic for a given fooling layer (cg is the final concentration when Jp_x is zero). Subsequently, the cumulative permeate volume as a function of time was estimated for each treatment.

2.5.2. Volume Reduction Factor (VCR)

The VCR, which indicates the degree of feed concentration resulting from permeate extraction through the membrane, was calculated according to Equation (2), where Vf corresponds to the initial feed volume and Vr to the final retentate volume [14].

$$\mathbf{VCR} = \frac{V_f}{V_r} = 1 + \left(\frac{V_p}{V_r}\right) \quad \text{(Eq. 3)}$$

2.5.3. Flux Decline Analysis

The decline Jp_{inst} was used to evaluate the impact of physical pretreatments on permeate flux. The first step consisted of comparing the GR+E and HS3+E treatments using 200 L of formulated raw juice as the feed volume.

Mathematical Procedure.

To quantitatively identify regime transitions and characterize Jp_{inst} decline kinetics, the following procedure was applied:

a) **Apparent decay coefficient.**

The instantaneous apparent Jp_{inst} decline coefficient (λ_i) was calculated as:

 doi:10.20944/preprints202606.0231.v1

$$\lambda_i = \left(\ln(j_i) - \ln(j_{i-1}) \Big/ t_i - t_{i-1} \right) \quad \text{(Eq. 4)}$$

where Ji and Ji−1 are the flux values at consecutive time points ti and ti−1, respectively.

b) **Smoothing.**

To reduce noise and enhance trend detection, λ was smoothed using a 5-point moving average.

c) **Segmentation and breakpoint detection.**

A segmented regression was applied to ln F(λ) to identify two transition times (t_{12} and t_{23}) corresponding to regime changes. The optimal breakpoints were determined by minimizing the total sum of squared errors (SSE) across three segments.

d) **Model fitting by regime**.

Based on the identified temporal boundaries, flux decline was modeled independently in each regime: based on the identified breakpoints, the filtration process was divided into three temporal regions:

Regime I: $0 < t \leq t_{12}$

Regime II: $t_{12} < t \leq t_{23}$

Regime III. $t > t_{23}$

Flux decline was modeled independently in each region using a piecewise formulation:

$$j_{(t)} = \begin{matrix} A\, e^{-k_1 t}, & 0 < t \leq t_{12} \\ a_2 + b_2 t, & t_{12} < t \leq t_{23} \\ a_3 + b_3 t, & t_{23} \end{matrix}$$

where:

A and K_1 are the exponential model parameters for Region I,

a_2, b_2 and a_3, b_3 are the linear regression coefficients for Regions II and III, respectively.

The productivity was calculated as: $AUC = \int_{t_i}^{t_f} j(t)dt$

The numerical analysis was done using the trapeze rule.

$$AUC_i = \frac{j_i + j_{i-1}}{2} (t_i - t_{i-1})$$

The Hermia models (Time-based forms) for the fouling mechanisms were applied [15]

Mechanism	Linearized form	Plot
Complete blocking	$\ln J = \ln J_0 - kt$	ln J vs t
Intermediate blocking	$1/J = 1/J_0 + kt$	1/J vs t
Standard blocking	$1/\sqrt{J} = 1/\sqrt{J_0} + kt$	$1/\sqrt{J}$ vs (t)
Cake filtration	$1/J^2 = 1/J_0^2 + kt$	1/J vs t

The R^2 was estimated after the linearization of J and t.

For the HS3+E CFM process for a long period, the same decline was applied for a feed volume of 300 and 400L to consider the CIP time within an industrial workday (8h). The same calculation procedure used to determine flux decline was consistently applied.

2.6. Particle Size Distribution

To evaluate the effect of GR and HS3 pretreatments before and after the enzymatic maceration on feed microstructure, the hydro pressed juice was characterized in terms of particle size distribution. Measurements were performed by laser diffraction using a mastersizer 3000 analyzer (Malvern Instruments Ltd., UK) equipped with a Hydro LV dispersion unit, following the protocol described by Dahdouh [16]. The optical parameters used were a refractive index of 1.45 for the dispersed phase (CSCG), 1.33 for water, an absorption index of 0.5, and an obscuration level of 11.24%.

 doi:10.20944/preprints202606.0231.v1

2.7. Quality Analysis

2.7.1. Physicochemical Analyses

Suspended insoluble solids (SIS) were quantified following the methodology described by [17]. Briefly, 15 g of sample were centrifuged at 5000 rpm for 10 min using a refrigerated centrifuge (SL16R, Thermo Scientific). The supernatant was carefully decanted and drained, and the remaining solid residue was considered the SIS fraction. All analyses were performed in triplicate.

2.7.2. Microbiological Analysis

Microbiological analyses were performed on the raw juice and permeate fractions corresponding to the clarified ready-to-drink Andean blackberry juice, following AOAC (2005) methods with minor modifications. Aerobic mesophilic bacteria were enumerated according to AOAC methods 988.18 and 990.12. Total and fecal coliforms were determined using AOAC method 2005.03. Yeasts and molds were quantified following AOAC methods 2002.11 and 997.02. All analyses were conducted in triplicate, and laboratory procedures were carried out in accordance with ISO 7218:2007 standards. The microbiological results were expressed as decimal logarithms of colony-forming units per milliliter (log CFU/mL), following standard recommendations for the handling and proper interpretation of microbiological data (AOAC International, 2005).

2.7.2. Sensory Analysis

The sensory properties of the samples were characterized through Quantitative Descriptive Analysis (QDA) in accordance with ISO 4121 standards. Eighteen semi-trained assessors (25–58 years of age) from the La Selva Research Center (Agrosavia, Colombia) participated in the evaluation. Panelists underwent five training sessions aimed at establishing a consensus of sensory vocabulary and ensuring consistent interpretation of attribute intensities. Samples were served at 8–10 °C in randomized, three-digit coded 30 mL cups and evaluated in individual booths under controlled environmental conditions. Sensory assessment was performed in morning and afternoon sessions, considering odor, taste, sensory sensations, and overall quality. The intensity of each attribute was scored on a structured 10-point scale (0 = not perceived; 10 = extremely intense). To reduce potential carryover effects, assessors rinsed their mouths with water between evaluations.

2.7.3. Bioactive Compounds Analysis

- **Reagents.**

All reagents used for analytical determinations were of analytical grade. Solvents used for UHPLC analyses were of HPLC grade. Methanol (purity ≥ 99.8%) and acetonitrile (LC/MS grade) were purchased from Merck (Germany), while formic acid was obtained from Sigma-Aldrich Chemie (Steinheim, Germany) and dimethyl sulfoxide (DMSO) from J.T. Baker. Ellagic acid and cyanidin-3-glucoside chloride (purity ≥ 98%) were supplied by PhytoLab GmbH & Co. Ultrapure water used in all analyses was produced using a Millipore Simplicity purification system.

Cyanidins and ellagitannins were extracted following the method of García-Villalba et al. (2015), with minor modifications adapted to the different matrices analyzed here. For raw and micro filtrated juices, 5 mL of sample were mixed with 5 mL of extraction solvent. For retentate, 5 mL of sample were extracted with two successive 10 mL solvent washes and adjusted to a final volume of 20 mL with methanol. The extraction solvent consisted of 0.5% (v/v) HCl in Type I water, methanol, and dimethyl sulfoxide in a 20:40:40 (v/v/v) ratio. Mixtures were agitated for 35 min, followed by centrifugation at 3000 rpm for 10 min at 20 °C. The supernatants were filtered through 0.22 µm nylon syringe filters and stored at −30 °C until chromatographic analysis. Quantification of cyanidins and ellagitannins was performed according to Mertz [18], with minor modifications, using a Vanquish UHPLC system (Thermo Scientific) equipped with a photodiode array detector. Chromatographic separation was achieved on a Hypersil Gold C18 reverse-phase column (100 × 2.1 mm, 1.9 µm; Merck,

 doi:10.20944/preprints202606.0231.v1

Germany) coupled to a guard column (10 × 2.1 mm, 1.9 µm). The mobile phase consisted of solvent A (water/formic acid, 98:2 v/v) and solvent B (water/acetonitrile/formic acid, 80:18:2 v/v/v), at a flow rate of 0.2 mL·min⁻¹ and a column temperature of 45 °C. The injection volume was 5 µL. The gradient program was as follows: 0 min, 5% B; 12 min, 15% B; 18 min, 30% B; 35 min, 25% B; 40 min, 5% B, followed by 5 min of re-equilibration. Detection wavelengths were set at 515 nm for cyanidins and 254 nm for ellagitannins. External calibration curves were constructed using cyanidin-3-glucoside (0.5–120 mg·L⁻¹; R^2 = 0.9995) and ellagic acid (5–300 mg·L⁻¹; R^2 = 0.9993). Cyanidin-3-rutinoside, lambertianin C, and sanguiin H-6 contents were expressed as equivalents of the corresponding external standards. All analyses were performed in triplicate.

- **Compounds retention.**

Amount of compound retention in the retentate, relative to the initial feed, was determined using Eq.5 according with [6] In this equation, C_p and C_r represent the solute concentrations in the permeate (p) and retentate (r), respectively, while V_p and V_r correspond to the total volumes of permeate (p) and retentate (r)

$$R\% = 100 * (\frac{Cr*Vr}{Cp}) * Vp \quad \text{(Eq. 5)}$$

2.8. Economic Evaluation Criteria for Andean Blackberry Juice Production

2.8.1. Energy Consumption

The electrical energy consumption of the equipment involved in the CFM processing line (see Figure 1) was estimated using Equation (7), based on the rated power provided in the technical datasheets and the operating time during the process.

$$\boldsymbol{Ee} = \boldsymbol{P} * \boldsymbol{t} / \eta \quad \text{(Eq. 6)}$$

where E is the electrical energy consumption, P is the power of the equipment (kW), t is the operating time (h), and η is motor efficiency.

Specific energy consumption (kW/L) was calculated in relation to the total volume of beverage obtained during the processing operation over a work shift.

2.8.2. Financial Indicators

For calculating the operating expenses (OPEX), we worked with a case study focused on technology transfer to rural communities. As the CFM process line was designed for implementation in small-scale agro-industries, this study was carried out in collaboration with an association of small growers named ASOFRUTAS (La Ceja, Antioquia, Colombia). First, a diagnosis of the infrastructure and service requirements (water, gas, electrical energy, see Figure 1) was conducted to estimate the investment necessary to strengthen the association's capacity for the optimal operation of the equipment.

In addition to the equipment investment, the analysis also considered the capital required to build the CFM unit and the other processing equipment, including auxiliary systems such as the boiler and compressor (see Figure 1), as well as the ultraclean packaging system, in order to estimate the total cost of producing blackberry juice in its final presentation. Moreover, the requirements for human resources, raw materials, packaging bags, productivity, and other operational factors were estimated for long-term process operation.

To assess profitability and investment recovery [19], the following economic sensitivity criteria were calculated:

2.8.2.1. Net Present Value (NPV) Analysis

The net present value (NPV) was calculated to evaluate the economic feasibility of the process, as defined by the following expression:

$$NPV = I0 + \sum_{\{t=1\}}^{\{n\}} \frac{\{CF_t\}}{\{(1+r)^t\}} \quad \text{(Eq. 7)}$$

 doi:10.20944/preprints202606.0231.v1

where: I0 is the initial capital investment, CFt = net cash flow at year t, r= discount rate, n= project lifetime (years) [20].

2.8.2.2. Internal Rate of Return (IRR)

The IRR is the discount rater that equates the present value of future cash flows to the initial investment, such that the NPV equals zero. Mathematically, project IRR is obtained by solving:

$$\boldsymbol{IRR} = \boldsymbol{-I0} + \sum_{\{t=1\}}^{\{n\}} \frac{\{\boldsymbol{CF_t}\}}{\{(\boldsymbol{1}+\boldsymbol{r})^{\boldsymbol{t}}\}} \quad \text{(Eq. 8)}$$

where: I_0= initial investment, CFt = net cash flow at year t, r= internal rate of return, n= project lifetime [21].

2.8.2.3. Payback Period

The time required for cumulative cash flows to equal the initial investment.

2.8.2.4. EBITDA

Financial ratios were used to assess the comparative valuation of the project

The EV/EBITDA ratio was calculated according to Equation (7):

$$\boldsymbol{EBIDTA} = \frac{\boldsymbol{EV}}{\{\boldsymbol{EBITDA}\}} \quad \text{(Eq. 9)}$$

where EV represents Enterprise Value and EBITDA corresponds to earnings before interest, taxes, depreciation, and amortization.

Similarly, the EV/Sales ratio was calculated as:

$$\frac{EV}{Sales}$$

where Sales represents total annual revenues.

2.9. Experimental Design

The study was designed to evaluate permeate flux behavior and process productivity under different feed physical preparation strategies and processing volumes. Two pretreatment conditions were assessed: GR+E and HS3+E. The GR+E treatment was evaluated at processing volumes of 100 and 200 L, whereas the HS3+E treatment was evaluated at 100, 200, 300 and 400 L to assess performance under extended operation conditions.

2.10. Statistical Analysis

Quality analysis was measured in triplicate, and results are reported as mean ± standard deviation (SD). Normality and homoscedasticity were verified with Shapiro–Wilk and Levene tests, respectively. For compound retention, a one-way ANOVA was conducted when significant differences were detected ($p < 0.05$), Tukey's HSD was used for pairwise comparisons. Sensory product characterization test was performed to identify discriminants with sensory descriptors according to the GR+E and HS3+E process treatment. For each descriptor, an ANOVA model was applied to check whether the scores given by the assessors differed significantly. All analyses were performed in XLSTAT (2023.1.4, Addinsoft, Paris, France).

3. Results and Discussion

3.1. Productivity

Figure 4 presents the temporal evolution of permeate flux for the GR+E and HS3+E treatments under crossflow microfiltration at the 200 L scale. In both cases, a characteristic flux decline pattern is observed, consisting of a rapid initial decrease followed by gradual stabilization over time, as has been published elsewhere and it is well known that membrane fouling is one of the main phenomena

 doi:10.20944/preprints202606.0231.v1

responsible for this [6], [22]. Previously, Zuluaga [9] reported higher flux (86 $L \cdot h^{-1} \cdot m^{-2}$) values for Andean blackberry juice under the same formulation (40% fruit content) and similar operating conditions (Pall microfiltration module, transmembrane pressure, and tangential velocity) working with a feed volume of 100L and a VFR of 7.7. The difference observed in this study may be explained by the fact that approximately twice the amount of raw material and feed juice volume was processed compared with the previous work. This likely resulted in a higher concentration of SIS, which contributed to increased membrane fouling as will be discussed later. In this regard, Behnaz Razi [23] indicated that suspended materials and cell debris accumulating on the membrane surface are responsible for permeate flux decline.

These results indicate that increasing production volume requires the implementation of strategies to maintain or enhance permeate flux over time. Retentate extraction (feed and bleed) during crossflow microfiltration has been reported to improve performance by limiting the accumulation of suspended solids, pectins, and colloids, thereby reducing viscosity, concentration polarization, and cake layer formation, key factors responsible for flux decline in fruit juice filtration [24]. Accordingly, a feed-and-bleed strategy was evaluated after the marked flux decline observed during the processing of 200L of feeding volume; however, no significant improvement in permeate flux was observed (see Appendix A.1), suggesting that fouling was mainly governed by rapid cake formation and pore blocking rather than bulk concentration effects. Therefore, strategies based solely on controlling retentate concentration of insoluble solids may be insufficient to mitigate fouling. Instead, modifying the physicochemical characteristics of the feed, particularly particle size distribution and structural organization, becomes critical.

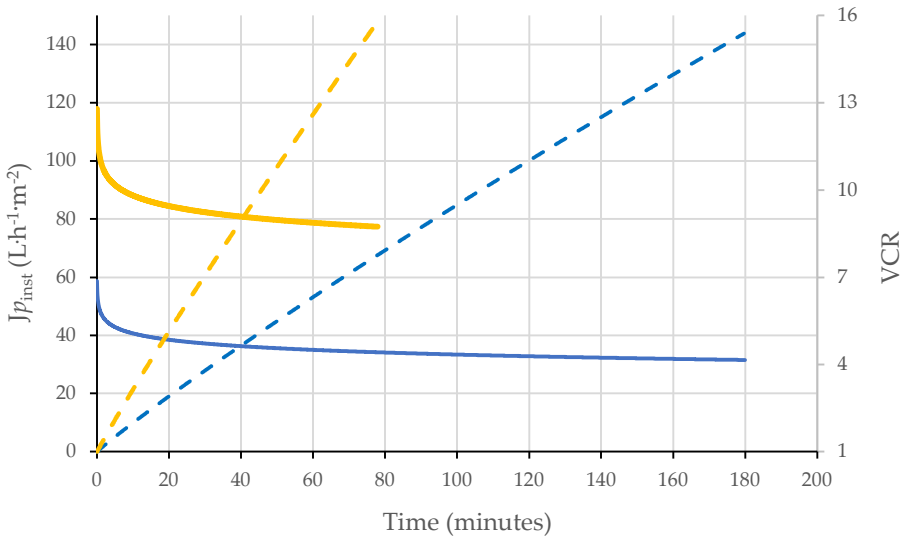

Figure 2. Flux decline dynamics of the GR+E and HS3+E treatments during crossflow microfiltration using a 200 L feed volume. Solid lines represent permeate flux (L.h-1.m-2), and dashed lines represent VCR. Blue lines correspond to GR+E treatment, while yellow lines correspond to HS3+E treatment. GR+E: screw-type grinder fitted with a 4.5 mm perforated plate. HS3+E: high-shear, three-stage rotor–stator inline homogenization treatment.

To further evaluate the impact of the HS3+E treatment, flux dynamics were analyzed by dividing the filtration process into distinct operational regions. The regime-segmented analysis summarized in Table 1 further quantifies these differences. Three distinct filtration regions were identified for both treatments, although their temporal boundaries differed. In regime 1, HS3+E showed a higher initial flux and a slower exponential decay rate compared to GR+E, suggesting reduced susceptibility to rapid pore blockage. In regime 2, both treatments exhibited a linear decline, but HS3+E maintained a

 doi:10.20944/preprints202606.0231.v1

higher average flux and a steeper slope, reflecting enhanced permeability under intermediate fouling conditions. In regime 3, corresponding to long-term operation, HS3+E continued to outperform GR+E, with higher final flux and cumulative productivity (AUC). Overall, the HS3+E treatment resulted in a substantial increase in process performance, with improvements in AUC ranging from approximately 110% to 158% across the three regimes

Table 1. Flux decline modeling parameters and performance metrics for GR+E and HS3+E treatments across filtration regimes.

Regime	1	2	3
Time GR+E (min)	0 – 6.83	6.83 – 46.49	46.49 – 179.95
Time HS3+E (min)	0 – 3.49	3.49 –21.33	21.33 – 77.9
Model GR+E	$J=46.94e^{-0.031t}$	J=38.95-0.13t	J=34.16-0.029t
Model HS3+E	$J=93.10e^{-0.025t}$	J=86.43-0.24t	J=82.49-0.057t
Initial Flux GR+E	46.94	38.05	32.79
Initial Flux HS3+E	93.1	85.58	81.27
Final flux GR+E	37.94	32.8	28.88
Final flux HS3	85.26	81.27	78.04
Average flux GR+E	42.3	35.42	30.84
Average flux HS3+E	89.13	83.43	79.65
AUC GR+E	288.92	1404.89	4115.54
AUC HS3+E	311.07	1488.36	4510.01

These observations are consistent with previous studies on crossflow microfiltration, which describe flux decline as a multi-stage process governed by evolving fouling mechanisms. Song [25] reported that flux decline typically transitions from an initial non-equilibrium regime to a pseudo-steady-state condition, driven by the progressive development of fouling layers. Similarly, Hermia [26], and subsequent studies [27], have demonstrated that early filtration stages are dominated by pore blocking mechanisms, while long-term behavior is controlled by cake formation and concentration polarization. In food systems such as fruit juice filtration, these mechanisms are particularly relevant due to the presence of suspended solids, colloids, and macromolecules that contribute to both internal and surface fouling.

From a mechanistic perspective, the improved performance observed for HS3 can be attributed to modifications in fouling behavior across the three regimes. In regime 1, the reduced rate of flux decline suggests that HS3+E mitigates pore blocking, likely by altering particle size distribution, reducing the presence of fine particulates, or modifying physicochemical interactions between solutes and the membrane surface. In regime 2, the higher flux and sustained decline indicate a more permeable and less compact fouling layer, which may result from changes in particle adhesivity, water retention capacity, or reduced compressibility of the cake layer. Finally, in regime 3, the higher steady-state flux observed for HS3+E suggests a dynamic equilibrium between fouling deposition and shear-induced removal, characteristic of crossflow systems, but shifted toward lower hydraulic resistance.

Overall, the combination of higher initial flux, slower decline, and increased cumulative productivity demonstrates that HS3+E significantly enhances filtration efficiency. The regime-based modeling approach further reveals that these improvements are not limited to a single stage but

 doi:10.20944/preprints202606.0231.v1

extend across all phases of the filtration process, highlighting the importance of controlling fouling mechanisms throughout operation.

3.2. Particle Size Distribution

The CFM process included size reduction using a GR, followed by an HS3, and subsequently an enzymatic maceration step. To evaluate the effect of HS3, the particle size distribution was analyzed in hydropressed samples before and after enzymatic maceration. Results show (Figure 5 and Table 2) that the GR with two peaks with biggest high size particles while the HS3 treatment was performed at a flow rate of 1.5 m³/h and 2900 rpm for 7 min. Considering a 30 kg batch and assuming a density close to 1 kg/L, the mixture passed through the rotor–stator system approximately six times. This repeated recirculation through the three-stage teeth configuration (coarse, middle, and fine, see appendix A2) promoted progressive particle disruption. The coarse stage favored initial tissue breakdown, the middle stage enhanced particle dispersion and refinement, and the fine stage contributed to further homogenization. As a result, the particle size distribution shifted toward smaller and more uniform particles, as observed in the solid blue curve in Figure 3. So, the particles sizes were highly reduced for the HS3 effect. After enzymatic maceration, the impact was evident on the particle size distribution, especially for the GR treatment (dotted blue line figure 5). For HS3 treatment the enzymatic maceration reduces the particle size for the main peak size from 170 µm to 135 µm and increased the particles of the minor size until 44% (see Figure 5 and Table 2).

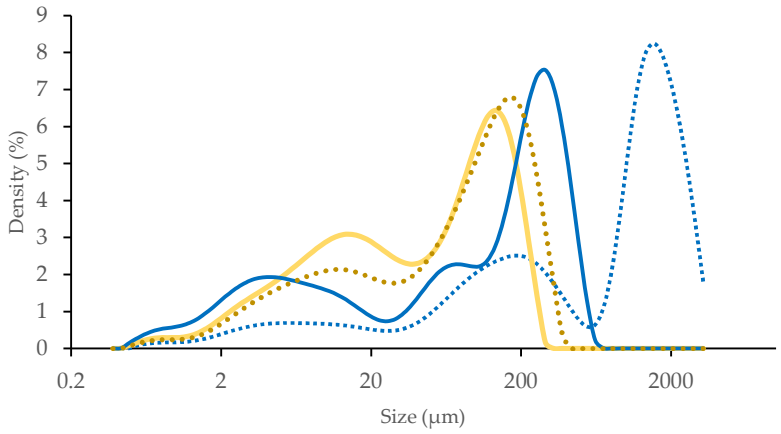

Figure 3. Particle size distribution of Andean blackberry hydro pressed juice. GR (blue point line): milling; GR+E: milling with enzymatic treatment (Blue compact line); HS3 (yellow point line): milling followed by homogenization using a three-stage rotor–stator system; HS3+E (Continue red line): milling and homogenization with a three-stage rotor–stator system combined with enzymatic treatment.

Table 2. Particle size (µm) distribution parameters of blackberry juice as affected by HS3 treatment and enzymatic maceration.

Treatment	Major peak	Density %	Min size	Max size	Minor peak 2	Density %	Min size	Max size
GR	1526.5	56.6	624.6	2890.9	15.4	31.3	29.2	549.8
GR+E	290.4	53.8	104.6	624.6	13.6	32.5	0.8	29.2
HS3	174.3	66.9	33.1	425.9	11.9	32.1	1.1	29.2
HS3+E	135.0	54.4	37.7	329.3	13.5	44.5	1.1	33.1

These structural modifications had a direct impact on filtration performance. From a mechanistic perspective, improved filtration performance can be explained by the changes in particle size distribution and structure induced by the HS3 treatment after the enzymatic hydrolysis. The presence

 doi:10.20944/preprints202606.0231.v1

of higher (290 μm main peak) particles in the GR-treated sample is known to promote pore blocking and internal fouling, leading to rapid flux decline and increased hydraulic resistance. In contrast, the reduction of fines and the formation of larger or aggregated particles (135 μm main peak) in the HS3+E treated sample favor the formation of a more porous and permeable cake layer, which reduces specific cake resistance and enhances flux stability [15]. Additionally, the application of high shear before enzymatic treatment likely enhances enzyme accessibility by increasing cell disruption and exposing intracellular components, including pectin. This can lead to more effective depectination, reducing viscosity and modifying inter-particle interactions and adhesivity to membrane material [28]; [29]. Lower viscosity and reduced pectin content are known to improve permeate flux in fruit juice microfiltration by decreasing resistance to flow and limiting the formation of dense fouling layers.

The Hermia analysis supports this interpretation, indicating that cake filtration is the dominant fouling mechanism for both treatments (R^2 up to 0.98). However, despite the similarity in the governing mechanism, the significantly higher flux observed for HS3+E demonstrates that the structure and permeability of the cake layer differ substantially between treatments. This confirms that fouling behavior is not only determined by the dominant mechanism but also by the physicochemical properties of the deposited layer.

These findings are consistent with previous studies. Song [25] described flux decline in crossflow microfiltration as a transition toward a cake-dominated regime, where the properties of the cake layer govern filtration performance. Similarly, Bacchin [30] highlighted the critical role of particle size and interactions in determining cake structure and permeability. In food systems, several authors have reported that reducing the fraction of fine particles and modifying pectin content significantly improves filtration performance by promoting the formation of less compact and more permeable fouling layers [31].

3.3. Effect of Processing Volume on Flux Performance of HS3+E-Treated Samples

Figure 4 shows the evolution of J_{px} for HS3+E-treated samples at processing volumes of 200, 300, and 400 L. In all cases, a similar flux decline pattern was observed, characterized by an initial rapid decrease followed by a gradual stabilization, indicating that the fundamental fouling behavior remains consistent across scales. However, clear differences in flux magnitude and decline kinetics were observed as a function of processing volume.

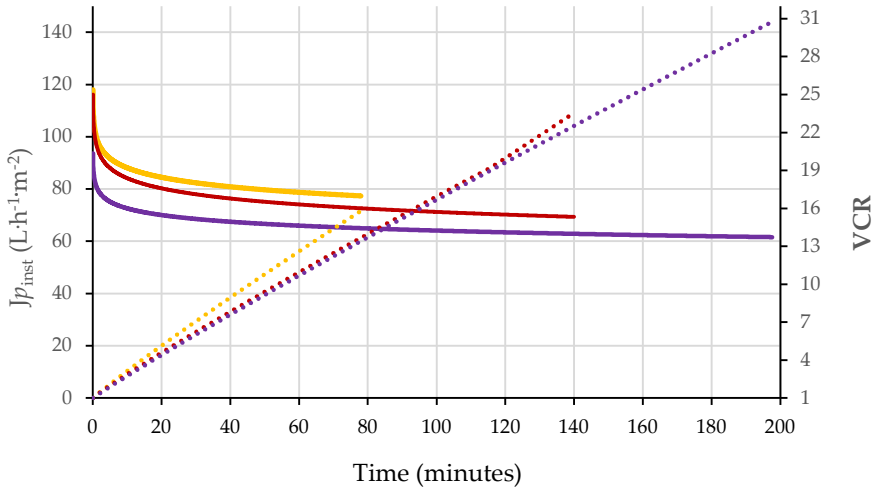

Figure 4. Effect of processing volumes HS-3+E on J_{px} during crossflow microfiltration of HS3+E-treated samples. Line colors: Yellow (200L), Red (300L), Purple (400L). The secondary axis represents the VCR achieved over time. The colors with points used for the VCR profiles correspond the same used for the J_{px} curves on the primary axis.

 doi:10.20944/preprints202606.0231.v1

The HS3+E-200 L condition exhibited the highest initial J_{px} ($L \cdot h^{-1} \cdot m^{-2}$), followed by HS3+E-300 L (93.1 $L \cdot h^{-1} \cdot m^{-2}$) and HS3+E-400 L (83.3 $L \cdot h^{-1} \cdot m^{-2}$), suggesting that an intermediate processing volume provides optimal conditions for feed structuring and filtration performance. Despite the lower initial flux at 400 L, all conditions converged toward similar steady-state flux values in the long-term regime 3, with average fluxes decreasing from 79.6 $L \cdot h^{-1} \cdot m^{-2}$ (200 L) to 63.5 $L \cdot h^{-1} \cdot m^{-2}$ (400 L), indicating increased resistance at larger volumes.

The regime-segmented analysis presented in Table 3 reveals that the transition times between filtration regimes increase with processing volume. Specifically, t23 increased from 21.3 min (200 L) to 50.9 min (400 L), while the duration of zone 3 expanded significantly from 56.6 min to 146.8 min. This indicates that at higher volumes, the system operates for longer periods under cake-dominated conditions, likely due to cumulative particle deposition and progressive cake growth.

Table 3. Regime-segmented flux decline parameters and productivity indicators for HS3+E-treated samples at different processing volumes (200–400 L).

Indicator	200	300	400
Regime transitions			
t_{12} (min)	3.5	4.9	6.6
t_{23} (min)	21.3	36.7	50.8
tmax (min)	77.9	139.9	197.6
Regime 3 (min)	56.6	103.2	146.8
Kinetic parameters			
J_0	93.1	102.1	83.3
k_1 (min^{-1})	0.03	0.04	0.02
B_2	−0.24	−0.31	−0.15
b_3	−0.06	−0.07	−0.03
Regime 3 performance			
Jstart,3	81.3	75.8	65.9
Jend,3	78.3	68.7	61.2
Average J_3	79.6	72.3	63.5
ΔJ3	3.2	7.1	4.7
J_f / J_0	0.8	0.7	0.7
Productivity			
AUC3	4507	7456	9328
AUCtotal	6292	10471	12882

The kinetic parameters further support this interpretation. The initial decay coefficient (k_1) remained within the same order of magnitude (0.02–0.04 min^{-1}), suggesting that early-stage fouling mechanisms are not strongly affected by the higher volume of juice processed. However, the slopes in regimes 2 and 3 (b_2, b_3) decreased in magnitude with increasing volume, particularly at 400 L, indicating a slower but more persistent flux decline associated with thicker and more resistant cake layers.

In terms of productivity, the cumulative permeate volume (AUC_3 and AUC_total) increased significantly with processing volume, reaching 12882 at 400 L compared to 6292 at 200 L. This reflects the extended filtration time and total processed volume, although it is accompanied by reduced flux efficiency. The ratio J_f / J_0 decreased from 0.8 (200 L) to 0.7 (300 L), indicating greater relative flux loss at intermediate scale, before slightly recovering at 400 L (0.7), suggesting a balance between fouling accumulation and hydrodynamic stabilization.

From a mechanistic perspective, the preservation of the regime 3 flux decline structure across all processed volumes confirms that fouling behavior is governed primarily by feed properties conditioned by the HS3+E treatment, rather than by the volume of juice processed. However, the shift in transition times and flux levels indicates that the higher volume of juice processed influences the extent and persistence of cake formation. Larger volumes likely promote increased particle residence time and cumulative deposition, leading to thicker and more compact fouling layers.

 doi:10.20944/preprints202606.0231.v1

These findings are consistent with classical crossflow microfiltration theory, which describes flux decline as a transition toward a cake-dominated regime controlled by particle deposition and shear-induced removal [25] [30]. Previous studies have also reported that, while the dominant fouling mechanism may remain unchanged during scale-up, the structure and resistance of the cake layer can vary due to differences in solids loading and operation time. In food systems, some authors like Cassano [7] and Vaillant [31] have shown that extended filtration times and higher feed loads lead to increased cake thickness and reduced permeability, in agreement with the trends observed in this study.

3.4. Effect of HS3+E Treatment on SIS and Separation Performance

The concentration of SIS in the raw juice and retentate for GR+E and HS3+E treatments is presented in Table 4. At a feeding volume of 200 L, the HS3+E-treated sample showed a significant ($p < 0.05$) lower SIS concentration in the raw juice (1.6) compared to the GR+E-treated sample (1.96), indicating that the combined high-shear treatment and enzymatic depectination effectively modified the particulate structure and dispersion of insoluble material. Despite operating at a similar VCR (15.4), the SIS content in the retentate for HS3+E was less than 50% of that observed for the GR+E treatment. This suggests that high-shear homogenization not only reduces SIS in raw juice. In contrast, the GR+E treatment retains a higher amount of insoluble material, which has a strong negative impact on permeate flux, as previously discussed.

Table 4. Effect of GR+E and HS3+E treatments on the distribution of suspended insoluble solids in raw juice and retentate during long-term crossflow microfiltration.

Treatment	Raw juice feeding volume	Suspends insoluble solids in raw juice	VCR	Suspends insoluble solids in retentate
GR+E	100	1.9±0.029a	7.7	4.1 ±0.058c
	200	1.9 ± 0.10a	15.4	7.1 ± 0.032a
HE3+E	100	1.5 ± 0.06c	7.7	1.9 ± 0.11e
	200	1.6 ± 0.05bc	15.4	3.1 ± 0.10d
	300	1.7 ± 0.03c	23.1	4.3 ± 0.23c
	400	1.7 ± 0.04b	30.3	4.9 ± 0.023b

The concentration factor (SIS_retentate /SIS_feed) further highlights these differences. For GR+E at 200 L, the concentration factor was approximately 3.62, while for HS3+E at the same volume it was approximately 1.91. This indicates that although both treatments lead to solids accumulation in the retentate, the HS3+E system significantly reduces the SIS concentration, likely due to its effect on cohesivity, adhesivity, swelling power etc. The lower SIS in the HS3+E feed suggests enhanced breakdown or restructuring of particulate matter during high-shear processing and enzymatic treatment.

When the feeding volume increased from 200 to 400 L under long-term CFM conditions with HS3+E treatment, the SIS concentration did not show a substantial increase (see Table 4). In the raw juice, only a slight rise was observed (from 1.65 to 1.70). For the retentate, the main increase occurred between 200 and 300 L, whereas at 400 L the change was limited to approximately 0.6 units. This is notable considering that the present long-term CFM experiments were conducted at significantly higher VCR values (23 and 30 for 300L and 400L, respectively).

Since the SIS in fruit juices act as primary foulants that readily contribute to membrane fouling, the reduction in SIS observed for the HS3+E treatment is relevant. This finding is consistent with previous studies on pretreatments in CFM processes, such as enzymatic depectinization, which enhances particle breakdown and reduces insoluble fractions in fruit juices. Studies by Vaillant [8], [10] have demonstrated that enzymatic treatments significantly improve clarification efficiency. However, the specific impact of the HS3+E treatment on SIS content, as well as its relationship with particle size distribution, has not been previously reported. Therefore, the results of this study support the hypothesis that high shear homogenization limits particle aggregation and reduces cake

 doi:10.20944/preprints202606.0231.v1

layer formation, both of which are key contributors to flux decline in crossflow microfiltration systems. In this context, the HS3+E treatment appears to modify not only the amount but also the nature of the suspended solids, resulting in a fouling layer that, although present, exhibits lower resistance to permeate flow. This explains why HS3+E-treated samples maintain higher flux and productivity even at increased processing volumes.

From a productivity standpoint, the reduction in particle size distribution and SIS achieved with the HS3+E treatment leads to a marked increase in cumulative processed volume during long-term CFM. As evidenced by the slopes of the regression lines in Figure 5, the GR treatment exhibits a significantly lower slope, achieving approximately 387 L of cumulative permeate over a 3-hour continuous process. Notably, while others CFM studies for fruit juices typically operate within a restricted VCR range, commonly between 5 and 11 Ramirez [32] [9], our results demonstrate high-intensity concentration up to a VCR of 30. In our experiments, we observed an exponential flux decrease in the initial phase (VCR 1.8 to 2.2), likely due to the rapid development of a concentration polarization layer, followed by a stabilized region that sustained productivity until the termination of the 180-minute run. This performance contrasts with traditional studies where permeate flux typically suffers from severe, continuous decline as concentration ratios increase [32] suggesting that the HS3+E treatment modifies the fouling layer's resistance, rendering it more permeable and amenable to high-intensity concentration.

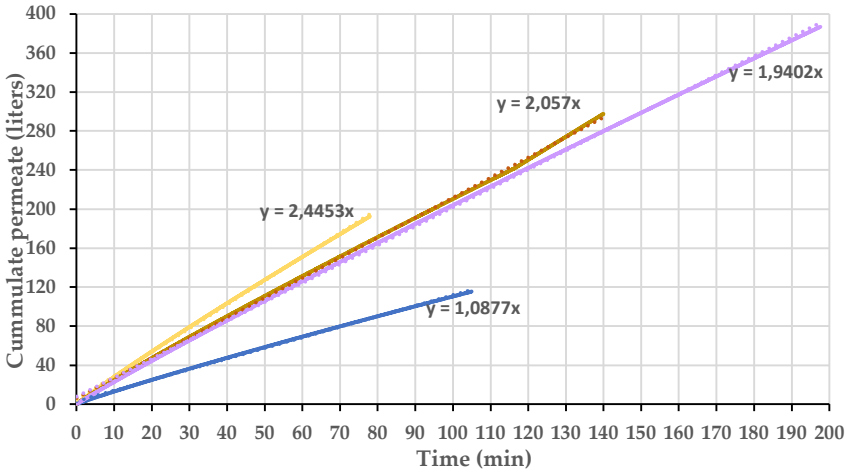

Figure 5. Cumulative permeates volume as a function of filtration time during the CFM process under different feeding volumes. HS3+E treatments: Yellow line: 200L, red line: 300L, purple line: 400L. Against the GR+E 200L treatment blue line.

3.5. Product Quality

3.5.1. Microbiology

Naturally, Andean blackberry exhibited a high initial microbial load, including molds and yeasts (5.80 ± 0.69 log CFU/mL), aerobic mesophiles (3.3 ± 0.68 log CFU/mL), lactic acid bacteria (3.27 ± 0.74 log CFU/mL), and total fecal coliforms (2.88 ± 0.69 log CFU/mL). These results are consistent with those reported by [33], which can be attributed to the climatic production conditions, the fruit's composition, and its fragile cell wall structure. The CFM process, coupled with an ultraclean packaging system, ensured a significant microbial reduction, with all microbiological quality indicators falling below the quantification limit of the analytical method (< $\log_{10}$ CFU/g). These findings are in agreement with [34] [35] Since the GR and HS3 are CFM pretreatments, they do not adversely affect microbiological quality of the final product; on the contrary, it contributed positively to the preservation of bioactive compounds as well as to the maintenance of fresh sensory attributes, as discussed later.

 doi:10.20944/preprints202606.0231.v1

3.5.2. Bioactive compound retention

The content and retention of bioactive compounds after CFM are presented in Table 5. For both treatments, GR+E and HS3+E, permeate concentrations were generally lower than those of the raw juice, whereas retentates showed similar or higher concentrations, indicating selective accumulation of some compounds in the retained fraction. This effect was particularly evident for Sanguiin H6 (SH6), whose concentration increased markedly in the retentate, while ellagic acid (EA) showed smaller differences among streams, suggesting a greater tendency to permeate the membrane.

Table 5. Content (mg/L) and retention (%) of cyanidins and ellagitannins during CFM.

Cyanidins (mg/L)				
	C3G[1]		**C3R[2]**	
Sample	**GR+E**	**HS3+E**	**GR+E**	**HS3+E**
Raw juice	95.7 ± 9.7	82.3 ± 1.3	90.5 ± 18.5	89.4 ± 14.7
MF* juice	88.8 ± 9.6	76.9 ± 2.3	73.6 ± 14.0	92.5 ± 13.0
Retentate	86.3 ± 17.9	92.4 ± 4.9	94.4 ± 5.9	93.7 ± 8.2
Retention (%)	10.0 ± 3.2a	4.2 ± 1.6b	12.2 ± 1.7a	4.3 ± 1.5b
Ellagitannins (mg/L)				
	SH6[3]		**EA[4]**	
Sample	**GR+E**	**HS3+E**	**GR+E**	**HS3+E**
Raw juice	36.1 ± 3.0	38.1 ± 8.0	11.9 ± 4.9	17.1 ± 3.6
MF juice	26.1 ± 12.8	24.2 ± 15.4	9.6 ± 2.0	24.1 ± 7.1
Retentate	70.5 ± 20.6	107.9 ± 25.8	7.3 ± 4.6	25.6 ± 6.6
Retention (%)	24.6 ± 14.9a	21.2 ± 11.6a	8.5 ± 2.6a	4.5 ± 2.1b

[1] Cyanidins 3 glucoside (external standard), [2] C3R: Cyanidin-3-glucose equivalent C3G. [3] SH6: Sanguiin H6 Ellagic Acid equivalent, [4] Ellagic Acid equivalent (external standard), MF*: microfiltered.

Bioactive compound retention was strongly affected by the upstream physical treatment applied before enzymatic depectination. In the GR+E treatment (VCR = 15.4), anthocyanins (C3G and C3R) showed moderate retention, whereas SH6 exhibited substantially higher retention than EA [9].

Similar behavior has been reported in berry juice microfiltration, where high-molecular-weight phenolics preferentially associate with suspended solids and are retained in the fouling layer [36] [37]. In contrast, HS3+E significantly reduced the retention of all bioactive compounds. Anthocyanin retention decreased to approximately 4.2%, while SH6 and EA retention reached 21.2% and 4.5%, respectively (Table 5). Consequently, about 95% of anthocyanins and 80% of ellagitannins were recovered in the permeate, representing an improvement over the recovery values typically reported for conventional fruit juice microfiltration systems [36][9].

The higher retention of SH6 is likely related to its large molecular weight (≈1869 Da) and its strong affinity for suspended solids and cell wall materials. Although these molecules are much smaller than the membrane pore size, retention is mainly governed by interactions with colloidal particles and fouling deposits rather than by size exclusion. Therefore, the lower retention observed in HS3+E suggests that high-shear homogenization reduced particle-associated retention mechanisms and limited fouling layer development [38] [39] [40].

Previous studies have demonstrated that fouling mitigation strategies, such as backpulsing or particle size reduction, significantly decrease the retention of anthocyanins and ellagitannins during crossflow [41] [9].

These findings are consistent with the higher permeate fluxes and productivity observed for HS3+E. By generating a finer and more homogeneous particle size distribution, homogenization promoted a less resistant fouling layer, improving mass transfer and enhancing the recovery of anthocyanins and ellagitannins [37][41]. Overall, the results demonstrate that pretreatment plays a critical role in controlling bioactive compound partitioning during CFM and that high-shear

 doi:10.20944/preprints202606.0231.v1

homogenization can improve both process performance and product quality under high volumetric concentration ratio conditions (VCR > 30), supporting the industrial feasibility of the process.

3.5.3. Sensory profile of microfiltered Andean blackberry juice.

The sensory profiles of microfiltered Andean blackberry juice produced from the GR+E and HS3+E treatments are presented in Figure 6. The HS3+E treatment does not adversely affect most sensory attributes of the microfiltered juice, including overall quality, blackberry flavor, sweetness, astringency, and sourness.

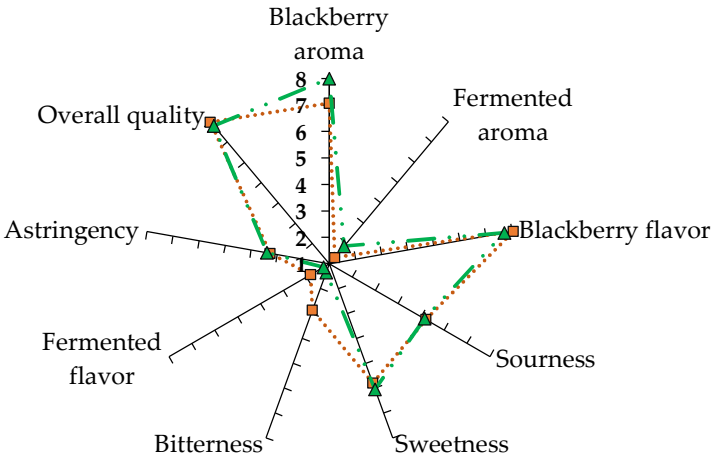

Figure 6. Sensory attribute profiles of microfiltered Andean blackberry juices produced using GR+E (orange squares) and HS3+E (green triangles) treatments.

Notably, the HS3+E treatment significantly enhanced blackberry aroma intensity compared to the GR+E ($p = 0.007$) and reduced the bitterness ($p < 0.0001$), contributing to a more balanced sensory perception that favors blackberry aroma and taste. This suggests that the high-shear process may promote the release or preservation of volatile compounds associated with fresh fruit aroma while improving overall flavor balance. This effect can be attributed to enhanced cellular disruption, which facilitates the release of aroma precursors and volatile compounds, as reported in fruit processing studies where mechanical treatments increase aroma availability through cell wall breakdown including volatiles, thereby intensifying aroma perception [42] [43] Moreover, high shear homogenization may liberate additional aroma precursors, such as glycosidic forms, which can be more readily cleaved by glycosidases typically present in commercial enzymatic cocktails. These findings indicate that the overall sensory balance of the juice was preserved, with improvements in aroma and taste. This is particularly relevant in an industrial context over the long term, as the results suggest that the inclusion of homogenization after milling in the CFM does not compromise the sensory quality of the product and may even contribute to a better balance of flavor and taste in the final product.

3.6. Economic Criteria for Blackberry Juice Production

The CMF process requires both electrical and thermal energy (see Figure 1). Thermal energy (used for sterilization and CIP procedures) was included in the cost calculations based on total plant

 doi:10.20944/preprints202606.0231.v1

process time. However, since the incorporation of HS3 does not affect the duration of these operations, the present analysis focuses on electrical energy consumption discussion.

3.6.1. Operational and energy performance under GR and HS3 configurations.

The operational performance of the GR and HS3 configurations was evaluated in terms of production capacity, specific energy consumption, and electricity cost per unit of processed beverage. As shown in Table 6, HS3 increased daily production from 187 to 387 L/day, corresponding to a 106.9% increase in throughput. This result indicates improved processability during downstream membrane operation, allowing the system to operate closer to installed capacity.

Table 6. Operational and energy performance of GR and HS3 configurations.

Metric	GR + E	HS3 + E	Difference
Daily production ($L.day^{-1}$)	187	387	200
Specific energy consumption ($kWh.L^{-1}$)	0.14	0.11	0.03
CFM stages energy consumption ($kWh.L^{-1}$)	0.08	0.06	0.02

At plant level, specific energy consumption decreased from 0.14 to 0.11 $kWh.L^{-1}$ (22.79%). Although HS3 introduced additional plant electrical demand (pump 5.4 kW and chiller 2.7 kW) associated with unit operation the higher production throughput reduced energy intensity per unit of processed beverage. When only CFM stage directly associated with membrane processing was considered, specific energy consumption decreased from 0.08 to 0.06 $kWh.L^{-1}$. These results confirm that HS3 improved membrane-stage energy efficiency rather than simply diluting fixed plant energy loads. The reduction in energy demand during HS3 + CFM operation suggests improved permeation stability, which could be associated with lower hydraulic resistance [11]. Similar behavior has been reported in membrane systems where process efficiency is strongly influenced by feed properties and fouling development during long-term operation [38], [13]. From a techno-economic perspective, this distinction is relevant because membrane operating costs depend basically on permeate productivity.

The results obtained for the CFM stages in the GR+E configuration were slightly higher than those reported for blackberry juices under the same configuration by [9]) (0.04 $kWh.L^{-1}$, average flux 80 $L{\cdot}h^{-1}{\cdot}m^{-2}$) and Gallego (0.07 $kWh.L^{-1}$, average flux 60 $L{\cdot}h^{-1}{\cdot}m^{-2}$). Those studies were conducted under short processing times (~1 h) and low VCR values (~11), whereas the GR+E configuration in the present study operated with feed volumes approximately twofold higher (200 L), which resulted in lower permeate flux values (33.7 $L{\cdot}h^{-1}{\cdot}m^{-2}$) at a VCR of 15.3, as discussed previously. The differences compared with the literature may be attributed to long-term process operation, in which flux decline becomes more pronounced over time. In addition, variations in process duration and operating conditions contribute to these discrepancies, as system behavior is inherently non-linear, making it difficult to extrapolate long-term performance from short-term experiments. Interestingly, when HS3 was applied, the average flux increased to 75 $L.h^{-1}.m^{-2}$ even at a higher VCR of 30. As a result, the specific energy consumption decreased significantly and reached values close to those reported by Gallego and Zuluaga. These findings demonstrate that the impact of homogenization is not limited to flux stabilization, but also that the process was ~22% more energy-efficient than the conventional particle size reduction process.

3.6.2. System-Level and Economic Implications

A detailed economic assessment was conducted considering operating expenditures including raw materials, process inputs, cleaning agents, filtration elements, and maintenance of key equipment (boiler, compressor, refrigeration unit, packaging system, and core processing line). Economic performance was evaluated using standard financial indicators NPV, IRR, payback period, and valuation multiples (EV/Sales and EV/EBITDA)—to assess profitability and investment feasibility under different process configurations [44]

 doi:10.20944/preprints202606.0231.v1

At system level (see Table 7), HS3 increased production (107%) capacity from 4,488 to 9,288 L/month without modifications to plant infrastructure, indicating that process limitations under GR conditions were primarily operational rather than capital-dependent.

Table 7. Techno-economic performance of the GR and HS3 configuration of CFM process line.

Indicator	GR+E	HS3+E	Difference
* Infrastructure invesment	104,036	104,036	0
* Process line equipment invesment	259,992	270,803	+10,811
* OPEX (month)	9,153	15,070	5,917
Monthly production in L	4488	9288	+4800
*Beverage production cost per L	3.92	2.84	−1.08
* Plant electricity cost per L	0.04	0.03	−0.01
* Monthly profit	5,282	7,910	+2,628
* NPV	−2,364	252	—
IRR (%)	NC	21	—
Payback period (months)	NC	60	—

* Values reported in USD; NC: Not calculable.

Blackberry beverage production cost decreased from 3.92 to 2.84 USD/L (27.55%) reflecting improved fixed-cost absorption and economies of scale. Although total OPEX increased (+64.6%), this rise is primarily driven by production scale rather than reduced efficiency, including higher raw material consumption, packaging, transportation, utility operation, and additional labor requirements. The HS3 configuration required five operators to support processing and handling activities, just one more worker than GR, contributing to the increase in labor-related operating costs. Despite this increase in OPEX, monthly profit increased from 5,282 to 7,910 USD/month (+49.76%), reflecting improved utilization of installed capacity. Economic feasibility indicators further supported the HS3 configuration. GR+E generated a negative NPV (−2,364 USD) and no calculable IRR, whereas HS3+E produced a positive NPV (252 USD), an IRR of 21%, and a payback period of 60 months. These improvements were achieved with only a 4.16% increase in machinery and equipment CAPEX, which related the cost of the HS3 equipment, while infrastructure investment remained unchanged.

Overall, the economic advantage of HS3 was primarily associated with increased throughput and improved membrane-stage efficiency rather than reductions in absolute plant electrical energy consumption. Overall, the results indicate that scale and capacity utilization are the dominant drivers of economic performance. These findings are consistent with previous studies highlighting energy and operating costs as key determinants of economic feasibility in juice processing systems [21, 45] [21], [45].

4. Conclusions

This study demonstrated that the productivity and techno-economic feasibility of CFM for Andean blackberry juice are strongly influenced by fouling dynamics associated with feed physicochemical characteristics generated during upstream processing. The conventional grinder treatment produced higher particle size distribution and suspended insoluble solids, leading to rapid

 doi:10.20944/preprints202606.0231.v1

and largely irreversible flux decline. In contrast, the incorporation of a high shear homogenization prior to enzymatic depectination significantly reduced particle size and SIS content, resulting in higher initial permeate flux, improved flux stability, and greater cumulative productivity during long-term operation, even at high volumetric reduction factors (VCR ≈ 30) and processing volumes up to 400 L. The regime-based flux analysis demonstrated that high-shear homogenization prior to enzymatic depectination improved process stability by delaying the onset of severe fouling and sustaining higher permeate fluxes during long-term operation. Importantly, HS3+E did not compromise product quality, ensuring microbial reduction while improving the recovery of anthocyanins and ellagitannins in the permeate. Sensory quality was also enhanced through reduced bitterness and increased Andean blackberry aroma. From a techno-economic perspective, HS3+E more than doubled production capacity, reduced beverage production cost and energy consumption, and achieved positive economic indicators, including a positive NPV, a 21% IRR, and a 60-month payback period, while the conventional GR+E configuration remained economically unfeasible. Overall, the results demonstrate that high-shear homogenization prior to enzymatic depectination is an effective strategy to improve process productivity, product quality, energy efficiency, and industrial feasibility of long-term CFM processing for small- and medium-scale agro-industrial applications.

Funding: The research has been funded by the Sistema General de Regalías (SGR) of the Departments of Antioquia and Caldas (Colombia), under Special Cooperation Agreement for Research No. 068 dated 10/08/2018. The OCAD of the "Fondo de Ciencia, Tecnología e Innovación (FCTeI)" designated the Corporación Colombiana de Investigación Agropecuaria – AGROSAVIA as the public executing entity for the project identified with BPIN code 2023000100074, titled "Desarrollo de la agroindustria rural, mediante la transferencia de tecnologías innovadoras de transformación, adaptables a los territorios de los departamentos de Antioquia y Caldas".

Data Availability Statement: The data that support the findings of this study are available from the corresponding author upon reasonable request.

Acknowledgments: The authors acknowledge the use of ChatGPT (OpenAI) during the preparation of this manuscript to improve language clarity, readability, and scientific writing. All content was carefully reviewed and edited by the authors, who take full responsibility for the accuracy and integrity of the published work. The authors sincerely acknowledge AGROSAVIA (Colombian Agricultural Research Corporation) and the National University of Colombia for their technical and logistical support throughout this study. Special thanks are also extended to the ASOFRUTAS association for its contribution to process validation under real operating conditions, and to BIOINTRIPIC for its support in the techno-economic assessment. The authors further express their gratitude to Adriana Vargas, Mariana Cabeza, Antonio Soto, Jhon Jaimes, Alfonso Cubillos, and Sergio Murcia for their valuable professional support and collaboration during the development of this research.

Conflicts of Interest: The authors declare no conflicts of interest.

Abbreviations

The following abbreviations are used in this manuscript:

BAC	Biologically active compounds
C3G	Cyanidin 3 glucoside molecule
C3R	Cyanidin 3 rutinoside molecule
CFM	Crossflow microfiltration
EA	Ellagic acid molecule
E_e	Electrical Energy
FJ	Formulated juice containing 40% fruit content
GR	Unit operation Grinder
GR+E	Grinder plus enzymatic treated juice process
HS3	Unit operation high-shear homogenization using a three-stage rotor–stator tri-emulsifying pump
HS3+E	Homogenizated plus enzymatic treated juice process
IRR	Internal Rate of Return

 doi:10.20944/preprints202606.0231.v1

Jp_{inst}	Adjusted flux
Jp_x	Permeate Flux ($L*h^{-1}*m^{2-1}$)
MFJ	permeate ready-to-drink blackberry juice
NPV	Net present value
R%	Solute Rejection
r	Retentate
SH6	Sanguiin H6
SIS	Suspended insoluble solids
TMP	Constant transmembrane pressure
VCR	Volumetric concentration ratio
η	Efficiency of electricity transmission.

Appendix A

Appendix A.1

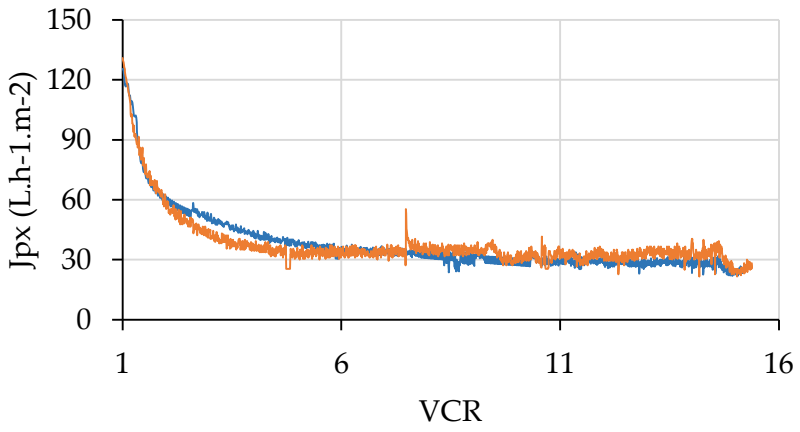

Figure A1. Flux behavior during the crossflow microfiltration process using a 200 L feed volume GR+E treatment, blue line. Feed-and-bleed strategy orange line.

Appendix A.2.

Figure A2. Three-stage rotor–stator tri-emulsifying pump (TRL-L3-60, Wenzhou Rayen Machinery Co., Ltd., China), powered by a 4.0 kW Siemens motor operating at 2900 rpm.

 doi:10.20944/preprints202606.0231.v1

References

1. Horvitz, S.; Chanaguano, D. Microbial and sensory quality of an Andean blackberry (Rubus glaucus Benth) cultivar. Acta Hortic. 2020, 1275, 121–124. https://doi.org/10.17660/ActaHortic.2020.1275.17.
2. Cardona-Hurtado, N.; Arrubla-Vélez, J.P.; Santa-Grajales, V. Valorization of agricultural byproducts from Rubus glaucus Benth (blackberry) as a natural source of high value-added ingredients. Biomass Conv. Bioref. 2026, 16, 82. https://doi.org/10.1007/s13399-025-06982-y.
3. Patras, A.; Brunton, N.P.; O'Donnell, C.; Tiwari, B.K. Effect of thermal processing on anthocyanin stability in foods: Mechanisms and kinetics of degradation. Trends Food Sci. Technol. 2010, 21, 3–11. https://doi.org/10.1016/j.tifs.2009.07.004.
4. Azofeifa, G.; Quesada, S.; Navarro, L.; Porras, O.; Arias, M.L. Pasteurization of blackberry juice preserves polyphenol-dependent inhibition of lipid peroxidation and intracellular radicals. J. Food Compos. Anal. 2015, 42, 56–62. https://doi.org/10.1016/j.jfca.2015.03.006.
5. Zia, H.; et al. A review study on the effects of thermal and non-thermal processing techniques on the sensory properties of fruit juices and beverages. Front. Food Sci. Technol. 2024, 4, 1405384. https://doi.org/10.3389/frfst.2024.1405384.
6. Castro-Muñoz, R.; Gómez-Aldapa, C.A.; Torres, A.C.; et al. Membrane technologies assisting plant-based and agro-food by-products processing: A comprehensive review. Trends Food Sci. Technol. 2020, 95, 219–232. https://doi.org/10.1016/j.tifs.2019.12.003.
7. Cassano, A.; Jiao, B.; Drioli, E. Clarification and concentration of citrus and carrot juices by integrated membrane processes. J. Food Eng. 2003, 57, 153–163. https://doi.org/10.1016/S0260-8774(02)00293-5.
8. Vaillant, F.; Millan, P.; Dornier, M.; Decloux, M.; Reynes, M. Strategy for economical optimisation of the clarification of pulpy fruit juices using crossflow microfiltration. J. Food Eng. 2001, 48, 83–90. https://doi.org/10.1016/S0260-8774(00)00145-3.
9. Zuluaga, J.; et al. Improving microfiltration efficiency of fruit beverages through backpulsing: Impact on permeate flux, cost-effectiveness and bioactive compounds retention. Sep. Sci. Technol. 2024. https://doi.org/10.1080/01496395.2024.2315609.
10. Pal-Verma, S.; Sarkar, B. Analysis of flux decline during ultrafiltration of apple juice in a batch cell. Food Bioprod. Process. 2015, 94, 147–157. https://doi.org/10.1016/j.fbp.2015.03.002.
11. Demoulin, C.; Dahdouh, L.; Ricci, J.; et al. Synergistic effect of particle size, shear rate and driving-force during microfiltration of fruit juices: Toward a relevant choice of pretreatments and filtration conditions. Innov. Food Sci. Emerg. Technol. 2023, 83, 103247. https://doi.org/10.1016/j.ifset.2022.103247.
12. Vaillant, F.; Jeanton, E.; Dornier, M.; O'Brien, G.M.; Reynes, M.; Decloux, M. Turbidity of pulpy fruit juice: A key factor for predicting cross-flow microfiltration performance. J. Membr. Sci. 2008, 325, 404–412. https://doi.org/10.1016/j.memsci.2008.08.015.
13. Dornier, M.; Belleville, M.-P.; Vaillant, F. Membrane Technologies for Fruit Juice Processing. In Fruit Preservation: Novel and Conventional Technologies; Rosenthal, A., Deliza, R., Welti-Chanes, J., Barbosa-Cánovas, G.V., Eds.; Springer: New York, NY, USA, 2018; pp. 203–230.
14. Conidi, C.; Castro-Muñoz, R.; Cassano, A. Membrane-Based Operations in the Fruit Juice Processing Industry: A Review. Beverages 2020, 6, 18. https://doi.org/10.3390/beverages6010018.
15. Pereira, G.L.D.; Cardozo-Filho, L.; Jegatheesan, V.; Guirardello, R. Generalization and expansion of the Hermia model for a better understanding of membrane fouling. Membranes 2023, 13, 290. https://doi.org/10.3390/membranes13030290.
16. Dahdouh, L.; Ricci, J.; Llauro, M.F.; et al. Influence of high shear rate on particle size, rheological behavior and fouling propensity of fruit juices during crossflow microfiltration: Case of orange juice. Innov. Food Sci. Emerg. Technol. 2018, 48, 304–312. https://doi.org/10.1016/j.ifset.2018.07.006.
17. Brito, B.; et al. Characterising polysaccharides in cherimoya (Annona cherimola Mill.) purée and their enzymatic liquefaction. Eur. Food Res. Technol. 2008, 226, 355–361. https://doi.org/10.1007/s00217-006-0547-2.
18. Mertz, C.; Cheynier, V.; Günata, Z.; Brat, P. Analysis of phenolic compounds in two blackberry species (Rubus glaucus and Rubus adenotrichus) by high-performance liquid chromatography with diode array

 doi:10.20944/preprints202606.0231.v1

detection and electrospray ion trap mass spectrometry. J. Agric. Food Chem. 2007, 55, 8616–8624. https://doi.org/10.1021/jf071475d.

19. Sinaga, A.S.; et al. Comparison of capital budgeting methods: NPV, IRR, Payback Period. World J. Adv. Res. Rev. 2023, 19, 1078–1081. https://doi.org/10.30574/wjarr.2023.19.2.1483.
20. Kehrein, P.; van Loosdrecht, M.C.M.; Osseweijer, P.; Garfí, M.; Dewulf, J.; Posada, J.A. A techno-economic analysis of membrane-based advanced treatment processes for the reuse of municipal wastewater. Water Reuse 2021, 11, 705–725. https://doi.org/10.2166/wrd.2021.016.
21. Laorko, A.; Tongchitpakdee, S.; Youravong, W. Economic Assessment for Cold Sterilization and Clarification of Pineapple Juice and Coconut Water Using Microfiltration. J. Appl. Membr. Sci. Technol. 2017, 21, 13–21. https://doi.org/10.11113/amst.v17i1.13.
22. Chiampo, F. Ultrafiltration to Increase the Consistency of Fruit Pulps: The Role of Permeate Flux. ChemEngineering 2024, 8, 3. https://doi.org/10.3390/chemengineering8010003.
23. Razi, B.; Aroujalian, A.; Fathizadeh, M. Modeling of fouling layer deposition in cross-flow microfiltration during tomato juice clarification. Food Bioprod. Process. 2012, 90, 841–848. https://doi.org/10.1016/j.fbp.2012.05.004.
24. Cissé, M.; Vaillant, F.; Acosta, O.; Perez, A.M.; Dornier, M.; Reynes, M. The quality of orange juice processed by coupling crossflow microfiltration and osmotic evaporation. Int. J. Food Sci. Technol. 2005, 40, 105–116. https://doi.org/10.1111/j.1365-2621.2004.00903.x.
25. Song, L.; Elimelech, M. Theory of concentration polarization in crossflow filtration. J. Chem. Soc. Faraday Trans. 1995, 91, 3389–3398. https://doi.org/10.1039/FT9959103389.
26. Hermia, J. Constant pressure blocking filtration laws—Application to power-law non-Newtonian fluids. J. Membr. Sci. 1982, 12, 285–300. https://doi.org/10.1016/S0376-7388(82)80062-4.
27. Field, R.W.; Wu, D.; Howell, J.A.; Gupta, B.B. Critical flux concept for microfiltration fouling. J. Membr. Sci. 1995, 100, 259–272. https://doi.org/10.1016/0376-7388(94)00265-Z.
28. Hwang, K.-J.; Hsu, C.-H.; Tung, K.-L. Effect of gel particle softness on the performance of cross-flow microfiltration. J. Membr. Sci. 2010, 364, 130–137. https://doi.org/10.1016/j.memsci.2010.08.043.
29. Salehi, F. Physico-chemical and rheological properties of fruit and vegetable juices as affected by food processing: A review. Int. J. Food Prop. 2020, 23, 1136–1149. https://doi.org/10.1080/10942912.2020.1781167.
30. Bacchin, P.; Aimar, P.; Field, R.W. Critical and sustainable fluxes: Theory, experiments and applications. J. Membr. Sci. 2006, 281, 42–69. https://doi.org/10.1016/j.memsci.2006.04.014.
31. Vaillant, F.; Millan, P.; O'Brien, G.; Dornier, M.; Decloux, M.; Reynes, M. Crossflow microfiltration of passion fruit juice after partial enzymatic liquefaction. J. Food Eng. 1999, 42, 215–224. https://doi.org/10.1016/S0260-8774(99)00124-7.
32. Ramírez, A.G.; et al. Optimization of the crossflow microfiltration of arazá juice (Eugenia stipitata) under different operation modes. Vitae 2011, 18, 153–161.
33. Horvitz, S.; Chanaguano, D.; Arozarena, I. Andean blackberries (Rubus glaucus Benth) quality as affected by harvest maturity and storage conditions. Sci. Hortic. 2017, 226, 293–301. https://doi.org/10.1016/j.scienta.2017.09.002.
34. Chaparro, L.; Castillo, S. Procesamiento de jugos de frutas empleando tecnología de membranas. Rev. Fac. Ing. UCV 2016, 31, 79–90.
35. Gallego-Ocampo, H.; Zuluaga, J.; et al. Integrated Microfiltration and Ultra-Clean Packaging for High-Quality Fruit Beverages in Rural Agro-Industries. Appl. Food Res. 2025, 5, 101496. https://doi.org/10.1016/j.afres.2025.101496.
36. Vladisavljević, G.T.; Vukosavljević, P.; Veljović, M.S. Clarification of red raspberry juice using microfiltration with gas backwashing: A viable strategy to maximize permeate flux and minimize loss of anthocyanins. Food Bioprod. Process. 2013, 91, 473–480. https://doi.org/10.1016/j.fbp.2013.04.004.
37. Urošević, T.; et al. Recent developments in microfiltration and ultrafiltration of fruit juices. Food Bioprod. Process. 2017, 106, 147–161. https://doi.org/10.1016/j.fbp.2017.09.009.
38. Cassano, A.; Donato, L.; Drioli, E. Ultrafiltration of kiwifruit juice: Operating parameters, juice quality and membrane fouling. J. Food Eng. 2007, 79, 613–621. https://doi.org/10.1016/j.jfoodeng.2006.02.020.

 doi:10.20944/preprints202606.0231.v1

39. Le Bourvellec, C.; Renard, C.M.G.C. Interactions between polyphenols and macromolecules: Quantification methods and mechanisms. Crit. Rev. Food Sci. Nutr. 2012, 52, 213–248. https://doi.org/10.1080/10408398.2010.499808.
40. Jakobek, L. Interactions of polyphenols with carbohydrates, lipids and proteins. Food Chem. 2015, 175, 556–567. https://doi.org/10.1016/j.foodchem.2014.12.013.
41. Cassano, A.; Conidi, C.; Drioli, E. Clarification and concentration of pomegranate juice (Punica granatum L.) using membrane processes. J. Food Eng. 2011, 107, 366–373. https://doi.org/10.1016/j.jfoodeng.2011.07.002.
42. Wu, W.; et al. Effects of high pressure and thermal processing on quality properties and volatile compounds of pineapple fruit juice. Food Control 2021, 130, 108293. https://doi.org/10.1016/j.foodcont.2021.108293.
43. Ravichandran, C.; Upadhyay, A.; Meda, V.; Rastogi, N.K.; Khan, Z.A.; Emanuel, N. Effect of high shear homogenisation on physicochemical, microstructure, particle size and volatile composition of residual pineapple pulp. Int. J. Food Sci. Technol. 2023, 58, 2092–2103. https://doi.org/10.1111/ijfs.15984.
44. Rodriguez-Gonzalez, O.; Buckow, R.; Koutchma, T.; Balasubramaniam, V.M. Energy requirements for alternative food processing technologies—Principles, assumptions, and evaluation of efficiency. Compr. Rev. Food Sci. Food Saf. 2015, 14, 536–554. https://doi.org/10.1111/1541-4337.12142.
45. Tamires, D.; Pereira, G.L.Z.; Martínez, J. Economic evaluation of a promising strategy for the extraction and concentration of bioactive compounds from passion fruit rinds. Food Bioprod. Process. 2025, 154, 536–545. https://doi.org/10.1016/j.fbp.2025.08.007.